Single-nucleus transcriptomics reveal stress-related prefrontal activation in Tourette disorder

Philip J Moos [1], Caterina Branca [1,2], Marco Bortolato [1,2]

1. Department of Pharmacology and Toxicology, College of Pharmacy, University of Utah, Salt Lake City, UT, USA
2. Department of Cellular and Systems Pharmacology, College of Pharmacy, University of Florida, Gainesville, FL, USA

Corresponding author:

Marco Bortolato, MD PhD
Dept. of Cellular and Systems Pharmacology
College of Pharmacy
University of Florida
MSB, Room P1-31
1345 Center Drive
Gainesville, FL 32603
USA
e-mail: mbortolato@ufl.edu

Running title: Transcriptional profile of DLPFC in Tourette Disorder

Keywords: Tourette disorder – tics - dorsolateral prefrontal cortex - single-nucleus transcriptomics – immediate early genes – stress responsive genes

ABSTRACT

Background: Tics are sudden, partially controllable motor or vocal events that arise from disruptions within cortico–striatal–thalamo–cortical circuits. Within this network, converging evidence implicates the dorsolateral prefrontal cortex (DLPFC) as an important cortical node supporting voluntary tic control. This region is critical for top-down regulation and is particularly sensitive to stress, raising the possibility that molecular vulnerabilities within the DLPFC may influence the capacity to suppress tics. However, the underlying cellular and molecular architecture remains poorly defined.

Methods: To address this gap, we conducted the first single-nucleus RNA sequencing analysis of postmortem DLPFC tissue from men with Tourette disorder (TD) and age-matched neurotypical controls.

Results: Overall cell-type proportions did not differ significantly between groups. In contrast, gene ontology analyses revealed broad upregulation of transcripts involved in protein synthesis, most prominently in microglia, oligodendrocytes, and interneurons. Among neuronal lineages, these changes were most pronounced in superficial and middle-layer pyramidal neurons and vasointestinal peptide-positive interneurons. To determine whether these alterations reflect engagement of stress-related transcriptional programs, we compared TD-associated differentially expressed genes with published single-nucleus datasets from major depressive disorder and posttraumatic stress disorder. Across DLPFC cell populations, and especially within pyramidal neurons and interneurons, we observed significant enrichment for stress-associated gene signatures, including glucocorticoid-responsive transcripts and immediate early genes.

Conclusion: Together, these findings identify the DLPFC in TD as a region of heightened stress responsivity and altered excitatory–inhibitory dynamics, offering new insight into cortical mechanisms that may constrain tic suppression.

INTRODUCTION

Tourette disorder (TD) is a neurodevelopmental condition characterized by multiple motor tics and at least one vocal tic persisting for more than one year (1). Tics are sudden, repetitive movements or vocalizations arising from dysfunction within cortico–striatal–thalamo–cortical (CSTC) circuits (2), and are thought to originate from aberrant "disinhibition foci" within the striatum (3), driven in part by loss of cholinergic and parvalbumin (PV)-positive GABAergic interneurons (4,5).

Tics are best conceptualized as "unvoluntary" behaviors (6), insofar as most individuals with TD retain a measurable capacity to transiently suppress them (7,8). The mechanism that permits this temporary suppression depends on prefrontal regions responsible for top-down control. In this network, the dorsolateral prefrontal cortex (DLPFC) has emerged as an important region for the voluntary regulation of tics. This region supports core executive functions, including working memory, response inhibition, and the flexible regulation of motor output (9–12). Notably, many individuals with TD exhibit executive deficits, which may contribute to difficulties regulating tic expression (13,14).

Functional imaging studies show increased DLPFC activation during tic suppression and other volitional inhibitory actions in TD (15,16). Disruptions in DLPFC structure or function have been linked to tic severity, supporting a central role for this region in implementing inhibitory control. However, an alternative perspective suggests that excessive DLPFC activation may enhance excitability in downstream motor regions and thereby contribute to tic expression (17).

A defining feature of the DLPFC is its marked susceptibility to stress (18). In primates, acute stress interferes with persistent firing through rapid catecholamine-driven weakening of dendritic spines, leading to diminished synaptic efficacy and compromised regulatory control (19,20). Acute stress interferes with this mode of signaling through rapid catecholamine-driven weakening of dendritic spines, leading to diminished synaptic efficacy and compromised regulatory control (18). This vulnerability is especially relevant to TD, as stress is among the most potent modulators of tic expression (21–23). Individuals with TD frequently report marked symptom exacerbation during periods of emotional strain, uncertainty, or cognitive overload (21,22). Physiological studies likewise demonstrate that stress alters CSTC activity in ways that can reduce the effectiveness of voluntary suppression (24).

Despite the central role of the DLPFC in tic control, its cellular and molecular involvement in TD remains poorly defined. Postmortem studies have focused primarily on subcortical structures, particularly the striatum, where alterations in interneuron populations, microglia, and dopaminergic signaling have been described (4,5,25,26) and corroborated by single-nucleus RNA sequencing (snRNA-seq) analyses (27). In contrast, it remains unclear which DLPFC cell types are most affected in TD, which molecular pathways are disrupted, and whether these changes align with mechanisms known to impair prefrontal regulation, including dysregulated protein synthesis, synaptic remodeling, or activation of stress-responsive transcriptional programs.

To address this gap, we conducted the first snRNA-seq analysis of postmortem DLPFC tissue from men with TD and age-matched neurotypical controls. This approach enables

high-resolution profiling of transcriptional states across individual cell nuclei and is well suited for studying the cellular diversity of the human prefrontal cortex (28). To assess whether TD-associated transcriptional changes reflect engagement of stress-related molecular programs, we compared TD differentially expressed genes (DEGs) with published single-nucleus datasets from major depressive disorder (MDD) and posttraumatic stress disorder (PTSD) (29), two conditions marked by heightened stress responsivity.

METHODS AND MATERIALS

The section below provides a concise summary of the experimental design, tissue provenance, and analytical framework. Full methodological details, including reagent lists, buffer compositions, sequencing parameters, quality-control thresholds, and computational pipelines, are provided in the Supplemental Material.

Human Brain Collection and Donor Information. Postmortem human brain tissue from the dorsolateral prefrontal cortex (DLPFC; Brodmann area 9, BA9) was obtained from the NIH NeuroBioBank Brain Tissue Resource Center at Harvard University. TD cases were collected through the Tourette Association of America. Control donors were screened to exclude psychiatric and neurological disorders. Cases with prolonged hypoxia or neuropathological abnormalities were excluded.

The cohort consisted of two age-matched male groups (n = 5 TD, n = 5 controls, Table 1) with no significant differences in age ($t(8)=0.14$, $P=0.89$) or postmortem interval (PMI, $t(8)=0.3$. $P=0.76$). Diagnoses were confirmed by trained research clinicians through structured family interviews and medical record review. Tissue donation was obtained with next-of-kin consent under NIH ethical guidelines. Frozen right-hemisphere tissue was coronally sectioned, and BA9 was identified using anatomical landmarks with exclusion of white matter.

Tissue Processing, Nuclei Isolation, and Sequencing. Nuclei were isolated from frozen BA9 tissue by mechanical homogenization followed by density-gradient purification under RNase-protected conditions. Purified nuclei were processed at the

Huntsman Cancer Institute High Throughput Genomics Core for 10x Genomics single-nucleus RNA sequencing library preparation and sequencing.

Data Processing, Cell Type Annotation, and Functional Analysis. Sequencing data were processed using the Cell Ranger pipeline (30) with alignment to the GRCh38 reference genome. Quality control, normalization, clustering, and downstream analyses were performed in Seurat. Low-quality nuclei, mitochondrial transcripts, and hemoglobin genes were excluded (31–36).

Cell-type annotation was performed using a custom human BA9 reference dataset derived from PsychENCODE (37) and implemented using the Azimuth framework (33). Differential gene expression was assessed using Wilcoxon rank-sum testing with false discovery rate correction. Functional pathway and Gene Ontology analyses were conducted using enrichR (version 3.4) (38–40).

Cross-Disorder Gene Overlap and Pseudotime Analysis. TD-associated DEGs were compared with published single-nucleus datasets from major depressive disorder (MDD) and posttraumatic stress disorder (PTSD) using gene overlap statistics. Neuronal maturation trajectories were analyzed using Monocle3 pseudotime modeling.

Statistical Analyses. All statistical analyses were conducted in R (version 4.4.2). Pseudotime comparisons were performed using the Wilcoxon rank-sum test. For GO analysis, genes with $P < 0.05$ were selected and the top 20 enriched pathways were visualized as heatmaps. Visualizations were generated using Seurat and ggplot2.

Results are presented as mean ± SEM, with significance set at $P < 0.05$ unless otherwise specified.

RESULTS

Sample collection and cell-type identification. Frozen BA9 samples were collected from 10 male individuals, including 5 with TD and 5 age-matched neurotypical controls. SnRNA-seq was performed on isolated nuclear fractions. One control subject was excluded due to insufficient RNA quality (Supplemental Fig. 1), yielding a total of 72,340 high-quality nuclei (29,159 from controls; 43,181 from TD samples).

Unsupervised clustering identified six major cell types (Figure 1A–B): pyramidal neurons (22,276 nuclei; 30.8%), interneurons (6,015; 8.3%), astrocytes (8,657; 12.0%), oligodendrocytes (26,321; 36.4%), oligodendrocyte precursor cells (OPCs; 4,392; 6.1%), and microglia (3,093; 4.3%). No significant differences in overall cell-type proportions were observed between TD and control samples (Figure 1C).

Broad transcriptional alterations in non-neuronal cell populations. Non-neuronal populations displayed widespread transcriptional dysregulation. Astrocytes (3,503 DEGs: 537 up, 2,966 down), oligodendrocytes (4,110 DEGs: 815 up, 3,295 down), and OPCs (926 DEGs: 167 up, 759 down) were dominated by downregulation, whereas microglia (733 DEGs: 428 up, 305 down) showed a balanced distribution (Supplemental Data 1-3).

Despite the prevalence of downregulated genes in several non-neuronal populations, GO enrichment analyses revealed that many of the most significant functional signatures were associated with upregulated genes (Figure 1D). Specifically, in neuronal populations, TD brains showed upregulation of *Global Translation*

(GO:0006412), *Macromolecule Biosynthetic Process* (GO:0009059), and *Cytoplasmic Translation* (GO:0002181), accompanied by structural enrichment in *Mitochondrial Inner Membrane* (GO:0005743) and *Neuron Projection* (GO:0043005), and functional increases in *GABA Receptor Activity* (GO:0016917) and *Ligand-Gated Anion Channel Activity* (GO:0099095) (Supplemental Fig. 2). Across non-neuronal populations, astrocytes and microglia showed elevated translation, ribosomal enrichment, and increased RNA- and ubiquitin-binding functions; oligodendrocytes also displayed heightened GABA receptor–related signaling; and OPCs exhibited a distinct profile enriched for *Response to Unfolded Protein* (GO:0006986), axon guidance, vesicle and growth cone structures and adenylate cyclase regulator activity. Together, these patterns indicate coordinated activation of protein synthesis pathways, coupled with structural and functional adaptations in mitochondrial, ribosomal, and synaptic components in TD brains.

Layer-specific remodeling of pyramidal neurons. The annotation of pyramidal neurons was conducted based on key layer-specific and subpopulation-specific markers, identifying six distinct clusters of pyramidal neurons (Figure 2A-B). Specifically, Layer 2-3 Superficial Intratelencephalic neurons (L2-3 Sup IT, n = 6,502; 24.8%), Layer 3-4 Middle Intratelencephalic neurons (L3-4 Mid IT, n = 7,091; 28.6%), Layer 5-6 Deep Intratelencephalic neurons (L5–6 Deep IT, n = 6,271; 29.5%), Layer 5/6 Near-Projecting neurons (L5/6 NP, n = 465; 2.1%), Layer 6 Corticothalamic neurons (L6 CT, n = 1,264; 7.5%), and Layer 6b neurons (L6b, n = 1,133; 7.5%). No significant

differences in cell-type proportions were observed between TD and control groups (Figure 2C).

Excitatory projection neurons in TD display pronounced layer-specific transcriptional remodeling (Supplemental Data S4-6). Deeper layers were characterized by a predominance of upregulated genes, with L5/6 Deep IT showing the largest number of changes (3,433 DEGs: 2,291 up, 1,142 down), followed by L5/6 NP (373 DEGs: 284 up, 89 down) and L6 CT (156 DEGs: 93 up, 63 down), all demonstrating a clear bias toward increased expression. In contrast, more superficial layers are dominated by downregulation, including L2-3 Sup IT (7,150 DEGs: 1,703 up, 5,447 down), L3-4 Mid IT (5,986 DEGs: 1,669 up, 4,317 down), and L6b (661 DEGs: 210 up, 451 down). These patterns reveal the coexistence of strongly upregulated programs in deeper layers and predominantly downregulated programs in superficial layers, reflecting distinct molecular remodeling across excitatory cortical circuits in TD.

To better understand the biological pathways underlying these expression shifts, we performed GO enrichment analyses (Figure 2D, Supplemental Fig. 3). Despite the predominance of downregulated genes in some subtypes, many of the most significant functional signatures were associated with upregulated genes. In TD brains, pyramidal neuron subtypes showed convergent activation of protein synthesis and mitochondrial pathways, alongside subtype-specific structural and functional changes. L3-4 mid and L2-3 sup IT neurons were enriched for *Translation* (GO:0006412), *Cytoplasmic Translation* (GO:0002181), and *Macromolecule Biosynthetic Process* (GO:0009059), with structural enrichment in ribosomal and mitochondrial membranes and functional increases in RNA binding, NADH dehydrogenase activity, and ubiquitin ligase

interactions. L5/6 NP neurons showed cytoplasmic translation, structural enrichment in microtubules, axonal growth cones, and ribosomes, and functional changes in cadherin binding, adenylate cyclase regulation, and GTP binding. L5-6 deep IT neurons were enriched for nervous system development and synaptic modulation, with structural changes in postsynaptic densities and membranes. L6 CT neurons displayed enrichment for synapse assembly and presynaptic membrane organization, while L6b neurons were characterized by calcium signaling-related processes, focal adhesion, and proton-transporting ATPase complexes, together with ubiquitin and adenylate cyclase regulator binding. Across excitatory neurons more broadly, common signatures included enhanced translation, mitochondrial function, and protein interaction pathways.

Widespread dysregulation in interneuron populations Within the interneuron population, two principal subgroups were distinguished: (1) medial ganglionic eminence (MGE)-derived interneurons, marked by LHX6 expression and further divided into parvalbumin-positive (PV+, n = 2,140; 34.0%) and somatostatin-positive (SST+, n = 1,927; 30.8%) cells; and (2) caudal ganglionic eminence (CGE)-derived interneurons, identified by PROX1 expression and classified as VIP+ (n = 1,060; 18.4%) or LAMP5+ (n = 888; 16.8%; Figure 3A–B). No significant differences in cell-type proportions were observed between TD and control groups (Figure 3C).

Interneuron populations in TD exhibit widespread transcriptional dysregulation (Supplemental Data S7-9), with a strong predominance of upregulated DEGs across all subtypes: VIP+ (566 DEGs: 515 up, 51 down), LAMP5+ (290: 263 up, 27 down), PV+ (1,415: 1,318 up, 97 down), and SST+ (525: 496 up, 29 down). GO enrichment

analyses revealed both shared and subtype-specific functional signatures (Figure 3D and Supplemental Fig. 4). VIP+ and LAMP5+ interneurons were dominated by upregulation of *Cytoplasmic Translation* (GO:0002181), *Peptide Biosynthetic Process* (GO:0043043), and *Macromolecule Biosynthetic Process* (GO:0009059), with structural enrichment in ribosomal components and molecular features such as RNA binding and ubiquitin-related interactions, consistent with increased protein synthesis and turnover. PV+ interneurons combined translational enrichment with *Oxidative Phosphorylation* (GO:0006119) and structural enrichment in mitochondrial membranes, supported by molecular signatures of NADH activity and oxidoreductive transport. In contrast, SST+ interneurons were enriched for protein quality control and regulatory processes, including *Regulation of Proteasomal Ubiquitin-Dependent Protein Catabolic Process* (GO:0032434) and *Protein Stabilization* (GO:0050821), with cellular component and molecular function enrichment patterns reflecting a focus on proteostasis rather than purely translational upregulation (Supplemental Fig. 4).

Pseudotime Trajectory Analysis. To investigate the differentiation pathways of excitatory and inhibitory neurons, we performed pseudotime analysis. Our findings showed that neurons from TD samples were predominantly found at earlier and intermediate maturation timepoints, contrasting with control neurons that advanced to later stages of pseudotime. While this developmental delay was most striking in pyramidal neurons (Supplemental Fig. 5A-C and Data S10), interneurons also exhibited a similar but less pronounced pattern (Supplemental Fig. 5D-F and Data S11), pointing

to impaired developmental progression in both major neuronal subtypes within TD conditions.

TD-associated transcriptional changes overlap with stress-related signatures in DLPFC. To evaluate whether the transcriptional alterations observed in the DLPFC of individuals with TD reflect broader stress-related molecular programs, we compared the DEGs identified in our dataset with published gene sets describing convergent molecular abnormalities in MDD and PTSD (29). Upon identification of the reference datasets, we first confirmed that cell-type cluster assignments were comparable across studies (Figure 4).

We observed substantial overlap between TD-associated DEGs and the shared MDD-PTSD gene set across multiple cortical cell populations (Figure 5, Supplemental Fig. 6-7, and Supplemental Data S12). The largest intersections of upregulated genes were found in pyramidal neurons and interneurons, where considerable proportions of TD-overexpressed genes also appeared in both stress-related disorders. Although the absolute number of shared genes was smaller in non-neuronal cell types, consistent enrichment was nevertheless evident in astrocytes, microglia, oligodendrocytes, and OPCs. These findings suggest that the TD transcriptional landscape recapitulates key components of stress-associated molecular dysregulation across both neuronal and glial compartments.

To determine whether these convergent gene sets mapped onto specific TD-defined cell clusters, we examined their distribution across our dataset. UMAP projections demonstrated that the shared MDD–PTSD signature was selectively enriched within the

same clusters exhibiting significant upregulation in TD (Figure 5 and Supplemental Fig.6).

Taken together, these analyses indicate that the DLPFC transcriptional architecture in TD is characterized by broad upregulation of genes previously implicated in stress-related psychopathology. The convergence across disorders, cell types, and analytic modalities supports the interpretation that chronic or dysregulated stress-adaptation mechanisms may represent a significant component of TD pathophysiology, particularly within excitatory and inhibitory cortical neurons.

To further delineate stress-responsive transcriptional dynamics in TD, we next examined whether TD-associated gene signatures overlapped with glucocorticoid-responsive modules identified by Chatzinakos et al., 2023 (29). In that study, dexamethasone exposure of iPSC-derived neurons yielded a well-defined set of corticosteroid-induced genes. Using these dexamethasone-responsive gene lists as a reference, we found widespread and robust transcriptional enrichment across all major DLPFC cell populations in TD (Figure 6A and Supplemental Data S13), indicating marked upregulation of corticosteroid-linked molecular pathways.

Cell-type-specific analyses revealed distinct yet convergent patterns of glucocorticoid-responsive gene induction. In neuronal populations, both pyramidal neurons and interneurons displayed increased expression of canonical immediate early genes (IEGs) together with metabolic and extracellular matrix regulators consistent with activity-dependent modulation and potential perisynaptic restructuring. Oligodendrocytes exhibited the strongest enrichment amongst the non-neuronal populations, with upregulation of osmotic and stress-adaptation genes such as *SLC5A3* and *HSPB1*,

pointing to alterations in white-matter homeostasis. Astrocytes showed elevations in growth factor–associated transcripts (*IGFBP7*), immediate early genes (*FOS*, *FOSB*), and cell-cycle regulators (*CKS2*), consistent with a reactive transcriptional phenotype. Microglia showed significant upregulation of stress-response machinery such as *HSP90AB1* and multiple DNA replication factors (*TOP2A*, *MELK*, *RRM2*), suggesting enhanced activation or remodeling states (Supplemental Data S13).

Given the prominence of glucocorticoid-responsive gene induction, we evaluated immediate early gene activity, a sensitive indicator of neuronal and glial activation. Using a curated IEG reference list (42), we identified strong enrichment across multiple TD cell populations, with the most pronounced activation signatures in microglia, followed by astrocytes and OPCs (Table 2 and Supplemental Data S14). A consistent pattern emerged across glial and neuronal compartments for the orphan nuclear receptor family genes *NR4A1*, *NR4A2*, and *NR4A3*, which regulate inflammatory responses, metabolic adaptation, and cellular stress resilience. Additional stress- and activity-associated transcripts, including *CCL2* in microglia and the IEGs *FOS*, *FOSB*, and *EGR1* across both neuronal and glial populations, were similarly elevated (Figure 6B and Supplemental Data S14).

Together, these findings demonstrate that the DLPFC in TD exhibits coordinated activation of glucocorticoid-responsive transcriptional modules and immediate early gene networks. The convergence of corticosteroid-induced signatures with activity-dependent gene enrichment across neuronal and glial compartments supports the presence of a generalized hyperactivated cortical state in TD and reinforces the involvement of stress-adaptation pathways in its underlying pathophysiology.

DISCUSSION

This study represents the first single-nucleus transcriptomic interrogation of the human DLPFC in TD. By profiling more than 72,000 nuclei across cortical neuronal and glial populations, we delineated a widespread transcriptional reorganization in TD that spans multiple cell classes. Specifically, our analysis revealed a distinctive molecular landscape marked by heightened translational activity, metabolic engagement, and robust induction of stress-responsive transcriptional programs. These findings collectively support a model in which the DLPFC in TD adopts a chronically stress-adapted molecular phenotype, reflecting sustained executive control demands and heightened stress sensitivity.

A striking feature emerging from the analysis is the absence of cell-type proportion differences between TD and neurotypical samples. All major cortical populations, including pyramidal neurons, interneurons, astrocytes, oligodendrocytes, microglia, and OPCs, were represented in comparable proportions across groups. This pattern contrasts with prior studies in the striatum, where reductions in cholinergic and PV-positive GABAergic interneurons have been documented (4,5). The absence of comparable cellular depletion in the DLPFC is in agreement with previous preliminary evidence indicating no differences in PV-positive GABAergic interneurons in the cingulate cortex of TD-affected individuals (41) and suggests that interneuron loss is unlikely to be a uniform feature across CSTC circuitry. Instead, TD may involve region-specific vulnerabilities, with subcortical structures showing discrete cytological alterations and prefrontal regions primarily exhibiting functional dysregulation but no

overt alteration in cellular architecture. Our results indicated profound alterations at the transcriptional level in the DLPFC. Both neuronal and glial populations exhibited widespread engagement of translational and biosynthetic programs. Pyramidal neurons, interneurons, astrocytes, and microglia displayed coordinated upregulation of protein synthesis pathways, ribosomal genes, mitochondrial components, and biosynthetic machinery. This pervasive activation of energetic and translational processes suggests that DLPFC circuits operate under sustained physiological load, consistent with neuroimaging evidence of heightened prefrontal recruitment in TD (43–45). These signatures likely reflect the chronic executive demands of tic suppression, which requires persistent engagement of prefrontal microcircuits and repeated activation of cognitive control networks (16,46). An alternative, though not mutually exclusive, possibility is that heightened DLPFC activity may itself potentiate excitability within downstream motor regions, thereby contributing to tic generation (17).

The relevance of these findings is underscored by the functional role of the DLPFC in TD. The DLPFC governs working memory, response inhibition, performance monitoring, and flexible regulation of motor output (11,47,48). These executive operations are essential for voluntary tic modulation, which relies on detecting premonitory urges, maintaining goal representations, and inhibiting tic-related motor patterns (49–51). Neuroimaging evidence shows increased DLPFC activation during deliberate tic suppression (15,16,52) and functional hyperactivation across TD cohorts (43–45), alongside atypical structural trajectories in children (53,54). The convergence of these observations with our transcriptional signatures suggests that the DLPFC in TD is

chronically over-recruited and undergoes sustained molecular adaptation linked to its compensatory role in regulating tics.

One of the most notable findings is the convergence between TD-associated DEGs and transcriptional signatures characteristic of MDD and PTSD (29). These disorders are defined by altered stress responsivity and dysregulated HPA axis function (55–57), both implicated in TD. Across neurons, astrocytes, microglia, and oligodendrocyte-lineage cells, TD samples exhibited upregulation of gene sets shared with MDD and PTSD, including genes involved in glucocorticoid signaling, mitochondrial metabolism, and synaptic modulation. This convergence suggests that chronic engagement of stress-response pathways is a defining feature of DLPFC dysregulation in TD.

The corticosteroid-responsive gene module from Chatzinakos et al., 2023 (29) was strongly enriched across all DLPFC cell types in TD. Genes induced by dexamethasone, a pharmacological mimic of sustained glucocorticoid exposure, were overexpressed in neuronal and glial populations alike. In particular, we documented a striking upregulation of IEG, such as *FOS*, *EGR1*, *NPAS4*, and *DUSP1* across pyramidal neurons, interneurons, as well as glia. IEGs are rapidly activated transcription factors that mark neuronal activity, synaptic remodeling, and cellular responses to salient stimuli (58–62). Their persistent activation in TD DLPFC suggests a state of heightened excitability and circuit engagement. Given that IEG induction can accompany both normal synaptic plasticity and maladaptive network overactivation (63), the widespread IEG profile likely indicates repeated recruitment of DLPFC microcircuits during tic suppression and stress exposure. Several IEG, including *NR4A1*, *NR4A2*, and

NR4A3, regulate mitochondrial dynamics, neuronal stress resilience, and metabolic adaptation. These transcription factors are key regulators of HPA axis feedback (64), and their consistent upregulation suggests chronic exposure of DLPFC cells to stress-related signals.

Robust IEG signatures were also observed in microglia and astrocytes, highlighting that stress- and activity-related signaling extends beyond neurons. Microglia also displayed pronounced induction of ribosomal transcripts, DNA replication factors, heat shock proteins, and inflammatory mediators. These signatures resemble reactive or remodeling states and align with evidence of microglial activation in TD (25,27,65). Given microglia's role in synaptic pruning and plasticity (66,67), chronic activation may reshape prefrontal synaptic architecture and alter excitatory–inhibitory balance. Astrocytes similarly exhibited enrichment for protein synthesis and stress-responsive genes. Together, these multicellular responses indicate that DLPFC networks in TD operate in a persistently activated physiological mode.

Taken together, these findings have implications for understanding the pronounced stress sensitivity of tic expression. Individuals with TD frequently report worsening tics during emotional strain, fatigue, uncertainty, or cognitive load (68–70). Children with TD show altered cortisol responsiveness under psychosocial stress, with evidence for heightened or dysregulated HPA axis activity (71,72). Preclinical studies further indicate that stress can precipitate tic-like behaviors and modulate CSTC circuit activity (21,73,74). Our transcriptional evidence of glucocorticoid and IEG activation provides a molecular substrate for these clinical observations, suggesting that DLPFC stress adaptation mechanisms are chronically engaged and may influence the capacity of

prefrontal circuits to regulate tics. Importantly, these mechanisms are likely to modulate tic expression rather than constitute a primary driver of tic generation itself, consistent with the role of the DLPFC as a modulatory node within CSTC circuitry rather than a core motor generator.

This interpretation is supported by the layer- and cell-type-specific patterns observed. Superficial pyramidal neurons displayed downregulation of genes related to synaptic stability and inhibitory control, whereas deeper-layer pyramidal neurons exhibited upregulation of genes associated with synaptic modulation and metabolic activation. VIP+ interneurons, which facilitate cortical disinhibition by suppressing SST interneurons (75–77), showed strong translational enrichment and activation of biosynthetic programs. These changes may promote excessive excitatory drive within DLPFC microcircuits, reducing inhibitory gating and undermining top-down control signals that suppress tics (15,16,78).

These stress-related transcriptional signatures may also bear on executive dysfunction in TD. Many individuals exhibit subtle deficits in working memory, cognitive flexibility, and inhibitory control (13,79,80), functions that depend on the stability of prefrontal microcircuits (48,81), which relies on intact dendritic spine architecture and finely tuned excitatory–inhibitory balance (82,83). Acute stress disrupts prefrontal function by weakening dendritic spines and impairing persistent firing (84–86), and chronic glucocorticoid signaling may similarly degrade prefrontal representations and compromise the executive control mechanisms required for effective tic suppression.

Several limitations should be considered. First, postmortem analyses cannot determine whether the transcriptional changes observed are causal or compensatory. Longitudinal animal studies will be required to resolve this issue. Second, snRNA-seq captures only nuclear transcripts and may not fully reflect cytoplasmic mRNA abundance or translational output. Finally, our cohort comprised only male donors, leaving open the question of whether similar signatures are present in females.

Despite these limitations, the present findings establish a foundation for understanding DLPFC involvement in TD at the cellular and molecular level. The convergence of stress-related transcriptional signatures with known executive deficits and stress sensitivity supports a model in which chronic engagement of stress-adaptive and activity-dependent pathways shapes the prefrontal contribution to tic expression. These findings may open avenues for research into the molecular mechanisms of tic suppression, and the development of novel interventions for TD. Future multimodal human and animal studies will be essential to test the causal roles of these pathways.

ACKNOWLEDGMENTS.

This study was partially supported by NINDS R21-NS125654. Postmortem human samples were obtained through the NIH NeuroBioBank from the Harvard Brain Tissue Resource Center/NIH NeuroBioBank. We acknowledge the Tourette Association of America (TAA) for spearheading, organizing and supporting the postmortem brain collection for patients with Tourette disorder. The authors thank Easton van Luik, Giulia Braccagni, and Teresa Musci for their assistance with the collection and processing of brain samples. The authors also acknowledge the Cancer Genomics Shared Resource and HCI's National Cancer Institute Center Support Grant (P30CA042014) and thank Dr. Brian Dalley and the staff for their assistance with the snRNA-seq experiments.

DISCLOSURES

The authors declare no conflict of interest.

DATA AND MATERIAL AVAILABILITY

All data needed to evaluate the conclusions in the paper are present in the paper and/or the Supplemental Materials. The data generated for snRNA-seq are available on Gene Expression Omnibus, GSE311334.

REFERENCES

1. American Psychiatric Association (Ed.) (2022): *Diagnostic and Statistical Manual of Mental Disorders: DSM-5-TR*, Fifth edition, text revision. Washington, DC: American Psychiatric Association Publishing.

2. Felling RJ, Singer HS (2011): Neurobiology of tourette syndrome: current status and need for further investigation. *J Neurosci* 31: 12387–12395.

3. Albin RL, Mink JW (2006): Recent advances in Tourette syndrome research. *Trends Neurosci* 29: 175–182.

4. Kalanithi PSA, Zheng W, Kataoka Y, DiFiglia M, Grantz H, Saper CB, *et al.* (2005): Altered parvalbumin-positive neuron distribution in basal ganglia of individuals with Tourette syndrome. *Proc Natl Acad Sci U S A* 102: 13307–13312.

5. Kataoka Y, Kalanithi PSA, Grantz H, Schwartz ML, Saper C, Leckman JF, Vaccarino FM (2010): Decreased number of parvalbumin and cholinergic interneurons in the striatum of individuals with Tourette syndrome. *J Comp Neurol* 518: 277–291.

6. Nilles C, Hartmann A, Roze E, Martino D, Pringsheim T (2023): Tourette syndrome and other tic disorders of childhood. *Handb Clin Neurol* 196: 457–474.

7. Leckman JF, King RA, Bloch MH (2014): Clinical Features of Tourette Syndrome and Tic Disorders. *J Obsessive Compuls Relat Disord* 3: 372–379.

8. Morand-Beaulieu S, Smith SD, Ibrahim K, Wu J, Leckman JF, Crowley MJ, Sukhodolsky DG (2022): Electrophysiological signatures of inhibitory control in children with Tourette syndrome and attention-deficit/hyperactivity disorder. *Cortex* 147: 157–168.

9. Barbey AK, Koenigs M, Grafman J (2013): Dorsolateral prefrontal contributions to human working memory. *Cortex* 49: 1195–1205.

10. Bissonette GB, Powell EM, Roesch MR (2013): Neural structures underlying set-shifting: roles of medial prefrontal cortex and anterior cingulate cortex. *Behav Brain Res* 250: 91–101.

11. Miller EK, Cohen JD (2001): An integrative theory of prefrontal cortex function. *Annu Rev Neurosci* 24: 167–202.

12. Ridderinkhof KR, Ullsperger M, Crone EA, Nieuwenhuis S (2004): The role of the medial frontal cortex in cognitive control. *Science* 306: 443–447.

13. Channon S, Pratt P, Robertson MM (2003): Executive function, memory, and learning in Tourette's syndrome. *Neuropsychology* 17: 247–254.

14. Eddy CM, Cavanna AE (2013): Altered social cognition in Tourette syndrome: nature and implications. *Behav Neurol* 27: 15–22.

15. Peterson BS, Skudlarski P, Anderson AW, Zhang H, Gatenby JC, Lacadie CM, *et al.* (1998): A functional magnetic resonance imaging study of tic suppression in Tourette syndrome. *Arch Gen Psychiatry* 55: 326–333.

16. Rae CL, Parkinson J, Betka S, Gouldvan Praag CD, Bouyagoub S, Polyanska L, *et al.* (2020): Amplified engagement of prefrontal cortex during control of voluntary action in Tourette syndrome. *Brain Commun* 2: fcaa199.

17. Jung J, Jackson SR, Parkinson A, Jackson GM (2013): Cognitive control over motor output in Tourette syndrome. *Neuroscience & Biobehavioral Reviews* 37: 1016–1025.

18. Joyce MKP, Uchendu S, Arnsten AFT (2025): Stress and Inflammation Target Dorsolateral Prefrontal Cortex Function: Neural Mechanisms Underlying Weakened Cognitive Control. *Biol Psychiatry* 97: 359–371.

19. Glausier JR, Datta D, Fish KN, Chung DW, Melchitzky DS, Lewis DA (2021): Laminar Differences in the Targeting of Dendritic Spines by Cortical Pyramidal Neurons and Interneurons in Human Dorsolateral Prefrontal Cortex. *Neuroscience* 452: 181–191.

20. González-Burgos G, Miyamae T, Krimer Y, Gulchina Y, Pafundo DE, Krimer O, *et al.* (2019): Distinct Properties of Layer 3 Pyramidal Neurons from Prefrontal and Parietal Areas of the Monkey Neocortex. *J Neurosci* 39: 7277–7290.

21. Godar SC, Bortolato M (2017): What makes you tic? Translational approaches to study the role of stress and contextual triggers in Tourette syndrome. *Neurosci Biobehav Rev* 76: 123–133.

22. Iverson KM, Litwack SD, Pineles SL, Suvak MK, Vaughn RA, Resick PA (2013): Predictors of Intimate Partner Violence Revictimization: The Relative Impact of Distinct PTSD Symptoms, Dissociation, and Coping Strategies. *Journal of Traumatic Stress* 26: 102–110.

23. Tan CY, Chiu N-C, Zeng Y-H, Huang J-Y, Tzang R-F, Chen H-J, *et al.* (2024): Psychosocial stress in children with Tourette syndrome and chronic tic disorder. *Pediatr Neonatol* 65: 336–340.

24. Conelea CA, Woods DW, Brandt BC (2011): The impact of a stress induction task on tic frequencies in youth with Tourette Syndrome. *Behav Res Ther* 49: 492–497.

25. Lennington JB, Coppola G, Kataoka-Sasaki Y, Fernandez TV, Palejev D, Li Y, *et al.* (2016): Transcriptome Analysis of the Human Striatum in Tourette Syndrome. *Biol Psychiatry* 79: 372–382.

26. Minzer K, Lee O, Hong JJ, Singer HS (2004): Increased prefrontal D2 protein in Tourette syndrome: a postmortem analysis of frontal cortex and striatum. *J Neurol Sci* 219: 55–61.

27. Wang Y, Fasching L, Wu F, Suvakov M, Huttner A, Berretta S, *et al.* (2025): Interneuron Loss and Microglia Activation by Transcriptome Analyses in the Basal Ganglia of Tourette Disorder. *Biological Psychiatry* 98: 260–270.

28. Herring CA, Simmons RK, Freytag S, Poppe D, Moffet JJD, Pflueger J, *et al.* (2022): Human prefrontal cortex gene regulatory dynamics from gestation to adulthood at single-cell resolution. *Cell* 185: 4428-4447.e28.

29. Chatzinakos C, Pernia CD, Morrison FG, Iatrou A, McCullough KM, Schuler H, *et al.* (2023): Single-Nucleus Transcriptome Profiling of Dorsolateral Prefrontal Cortex: Mechanistic Roles for Neuronal Gene Expression, Including the 17q21.31 Locus, in PTSD Stress Response. *Am J Psychiatry* 180: 739–754.

30. Zheng GXY, Terry JM, Belgrader P, Ryvkin P, Bent ZW, Wilson R, *et al.* (2017): Massively parallel digital transcriptional profiling of single cells. *Nat Commun* 8: 14049.

31. Butler A, Hoffman P, Smibert P, Papalexi E, Satija R (2018): Integrating single-cell transcriptomic data across different conditions, technologies, and species. *Nat Biotechnol* 36: 411–420.

32. Hao Y, Stuart T, Kowalski MH, Choudhary S, Hoffman P, Hartman A, *et al.* (2024): Dictionary learning for integrative, multimodal and scalable single-cell analysis. *Nat Biotechnol* 42: 293–304.

33. Hao Y, Hao S, Andersen-Nissen E, Mauck WM, Zheng S, Butler A, *et al.* (2021): Integrated analysis of multimodal single-cell data. *Cell* 184: 3573-3587.e29.

34. Romanov RA, Tretiakov EO, Kastriti ME, Zupancic M, Häring M, Korchynska S, *et al.* (2020): Molecular design of hypothalamus development. *Nature* 582: 246–252.

35. Satija R, Farrell JA, Gennert D, Schier AF, Regev A (2015): Spatial reconstruction of single-cell gene expression data. *Nat Biotechnol* 33: 495–502.

36. Stuart T, Butler A, Hoffman P, Hafemeister C, Papalexi E, Mauck WM, *et al.* (2018, November 2): Comprehensive integration of single cell data. https://doi.org/10.1101/460147

37. Zintel T (2022): Cellular Diversity in Human Subgenual Anterior Cingulate and Dorsolateral Prefrontal Cortex by Single-Nucleus RNA-sequencing. Synapse. https://doi.org/10.7303/SYN48374287.1

38. Chen EY, Tan CM, Kou Y, Duan Q, Wang Z, Meirelles GV, *et al.* (2013): Enrichr: interactive and collaborative HTML5 gene list enrichment analysis tool. *BMC Bioinformatics* 14: 128.

39. Kuleshov MV, Jones MR, Rouillard AD, Fernandez NF, Duan Q, Wang Z, *et al.* (2016): Enrichr: a comprehensive gene set enrichment analysis web server 2016 update. *Nucleic Acids Res* 44: W90–W97.

40. Xie Z, Bailey A, Kuleshov MV, Clarke DJB, Evangelista JE, Jenkins SL, *et al.* (2021): Gene Set Knowledge Discovery with Enrichr. *Current Protocols* 1: e90.

41. Vaccarino, Kataoka-Sasaki, Lennington (2013): Cellular and molecular pathology in Tourette syndrome. *Tourette Syndrome*. Oxford University Press, pp 205–220.

42. Wu YE, Pan L, Zuo Y, Li X, Hong W (2017): Detecting Activated Cell Populations Using Single-Cell RNA-Seq. *Neuron* 96: 313-329.e6.

43. Baym CL, Corbett BA, Wright SB, Bunge SA (2008): Neural correlates of tic severity and cognitive control in children with Tourette syndrome. *Brain* 131: 165–179.

44. Marsh R, Zhu H, Wang Z, Skudlarski P, Peterson BS (2007): A developmental fMRI study of self-regulatory control in Tourette's syndrome. *Am J Psychiatry* 164: 955–966.

45. Polyanska L, Critchley HD, Rae CL (2017): Centrality of prefrontal and motor preparation cortices to Tourette Syndrome revealed by meta-analysis of task-based neuroimaging studies. *Neuroimage Clin* 16: 257–267.

46. Ganos C, Kahl U, Brandt V, Schunke O, Bäumer T, Thomalla G, *et al.* (2014): The neural correlates of tic inhibition in Gilles de la Tourette syndrome. *Neuropsychologia* 65: 297–301.

47. Badre D, Wagner AD (2007): Left ventrolateral prefrontal cortex and the cognitive control of memory. *Neuropsychologia* 45: 2883–2901.

48. Robbins TW, Arnsten AFT (2009): The neuropsychopharmacology of fronto-executive function: monoaminergic modulation. *Annu Rev Neurosci* 32: 267–287.

49. Cavanna AE, Black KJ, Hallett M, Voon V (2017): Neurobiology of the Premonitory Urge in Tourette's Syndrome: Pathophysiology and Treatment Implications. *J Neuropsychiatry Clin Neurosci* 29: 95–104.

50. Ganos C, Kahl U, Schunke O, Kühn S, Haggard P, Gerloff C, *et al.* (2012): Are premonitory urges a prerequisite of tic inhibition in Gilles de la Tourette syndrome? *J Neurol Neurosurg Psychiatry* 83: 975–978.

51. Leckman JF, Walker DE, Cohen DJ (1993): Premonitory urges in Tourette's syndrome. *Am J Psychiatry* 150: 98–102.

52. Bohlhalter S, Goldfine A, Matteson S, Garraux G, Hanakawa T, Kansaku K, *et al.* (2006): Neural correlates of tic generation in Tourette syndrome: an event-related functional MRI study. *Brain* 129: 2029–2037.

53. Peterson BS, Staib L, Scahill L, Zhang H, Anderson C, Leckman JF, *et al.* (2001): Regional brain and ventricular volumes in Tourette syndrome. *Arch Gen Psychiatry* 58: 427–440.

54. Yamamuro K, Ota T, Iida J, Nakanishi Y, Uratani M, Matsuura H, *et al.* (2015): Prefrontal dysfunction in pediatric Tourette's disorder as measured by near-infrared spectroscopy. *BMC Psychiatry* 15: 102.

55. Bale TL (2006): Stress sensitivity and the development of affective disorders. *Hormones and Behavior* 50: 529–533.

56. Morris MC, Compas BE, Garber J (2012): Relations among posttraumatic stress disorder, comorbid major depression, and HPA function: a systematic review and meta-analysis. *Clin Psychol Rev* 32: 301–315.

57. Pariante CM, Lightman SL (2008): The HPA axis in major depression: classical theories and new developments. *Trends Neurosci* 31: 464–468.

58. Flavell SW, Greenberg ME (2008): Signaling mechanisms linking neuronal activity to gene expression and plasticity of the nervous system. *Annu Rev Neurosci* 31: 563–590.

59. Guzowski JF, Timlin JA, Roysam B, McNaughton BL, Worley PF, Barnes CA (2005): Mapping behaviorally relevant neural circuits with immediate-early gene expression. *Curr Opin Neurobiol* 15: 599–606.

60. Lanahan A, Worley P (1998): Immediate-early genes and synaptic function. *Neurobiol Learn Mem* 70: 37–43.

61. Minatohara K, Akiyoshi M, Okuno H (2015): Role of Immediate-Early Genes in Synaptic Plasticity and Neuronal Ensembles Underlying the Memory Trace. *Front Mol Neurosci* 8: 78.

62. Pérez-Cadahía B, Drobic B, Davie JR (2011): Activation and function of immediate-early genes in the nervous system. *Biochem Cell Biol* 89: 61–73.

63. Gallitano AL (2020): Editorial: The Role of Immediate Early Genes in Neuropsychiatric Illness. *Front Behav Neurosci* 14: 16.

64. Helbling J-C, Minni AM, Pallet V, Moisan M-P (2014): Stress and glucocorticoid regulation of NR4A genes in mice. *J Neurosci Res* 92: 825–834.

65. Frick L, Pittenger C (2016): Microglial Dysregulation in OCD, Tourette Syndrome, and PANDAS. *Journal of Immunology Research* 2016: 1–8.

66. Paolicelli RC, Bolasco G, Pagani F, Maggi L, Scianni M, Panzanelli P, *et al.* (2011): Synaptic Pruning by Microglia Is Necessary for Normal Brain Development. *Science* 333: 1456–1458.

67. Schafer DP, Lehrman EK, Kautzman AG, Koyama R, Mardinly AR, Yamasaki R, *et al.* (2012): Microglia sculpt postnatal neural circuits in an activity and complement-dependent manner. *Neuron* 74: 691–705.

68. Bornstein RA, Stefl ME, Hammond L (1990): A survey of Tourette syndrome patients and their families: the 1987 Ohio Tourette Survey. *J Neuropsychiatry Clin Neurosci* 2: 275–281.

69. Conelea CA, Woods DW (2008): The influence of contextual factors on tic expression in Tourette's syndrome: a review. *J Psychosom Res* 65: 487–496.

70. Lin H, Katsovich L, Ghebremichael M, Findley DB, Grantz H, Lombroso PJ, *et al.* (2007): Psychosocial stress predicts future symptom severities in children and adolescents with Tourette syndrome and/or obsessive-compulsive disorder. *J Child Psychol Psychiatry* 48: 157–166.

71. Buse J, Kirschbaum C, Leckman JF, Münchau A, Roessner V (2014): The Modulating Role of Stress in the Onset and Course of Tourette's Syndrome: A Review. *Behav Modif* 38: 184–216.

72. Corbett BA, Mendoza SP, Baym CL, Bunge SA, Levine S (2008): Examining cortisol rhythmicity and responsivity to stress in children with Tourette syndrome. *Psychoneuroendocrinology* 33: 810–820.

73. Godar SC, Mosher LJ, Strathman HJ, Gochi AM, Jones CM, Fowler SC, Bortolato M (2016): The D1CT-7 mouse model of Tourette syndrome displays sensorimotor gating deficits in response to spatial confinement. *Br J Pharmacol* 173: 2111–2121.

74. Godar SC, Mosher LJ, Di Giovanni G, Bortolato M (2014): Animal models of tic disorders: a translational perspective. *J Neurosci Methods* 238: 54–69.

75. Lee AT, Gee SM, Vogt D, Patel T, Rubenstein JL, Sohal VS (2014): Pyramidal neurons in prefrontal cortex receive subtype-specific forms of excitation and inhibition. *Neuron* 81: 61–68.

76. Pfeffer CK, Xue M, He M, Huang ZJ, Scanziani M (2013): Inhibition of inhibition in visual cortex: the logic of connections between molecularly distinct interneurons. *Nat Neurosci* 16: 1068–1076.

77. Pi H-J, Hangya B, Kvitsiani D, Sanders JI, Huang ZJ, Kepecs A (2013): Cortical interneurons that specialize in disinhibitory control. *Nature* 503: 521–524.

78. Wang Z, Maia TV, Marsh R, Colibazzi T, Gerber A, Peterson BS (2011): The neural circuits that generate tics in Tourette's syndrome. *Am J Psychiatry* 168: 1326–1337.

79. Eddy CM, Rizzo R, Gulisano M, Agodi A, Barchitta M, Calì P, *et al.* (2011): Quality of life in young people with Tourette syndrome: a controlled study. *J Neurol* 258: 291–301.

80. Morand-Beaulieu S, Grot S, Lavoie J, Leclerc JB, Luck D, Lavoie ME (2017): The puzzling question of inhibitory control in Tourette syndrome: A meta-analysis. *Neurosci Biobehav Rev* 80: 240–262.

81. Goldman-Rakic PS (1995): Architecture of the prefrontal cortex and the central executive. *Ann N Y Acad Sci* 769: 71–83.

82. Gonzalez-Burgos G, Miyamae T, Pafundo DE, Yoshino H, Rotaru DC, Hoftman G, *et al.* (2015): Functional Maturation of GABA Synapses During Postnatal Development of the Monkey Dorsolateral Prefrontal Cortex. *Cereb Cortex* 25: 4076–4093.

83. Lewis DA, Hashimoto T, Volk DW (2005): Cortical inhibitory neurons and schizophrenia. *Nat Rev Neurosci* 6: 312–324.

84. Arnsten AFT (2015): Stress weakens prefrontal networks: molecular insults to higher cognition. *Nat Neurosci* 18: 1376–1385.

85. Arnsten AFT (2009): Stress signalling pathways that impair prefrontal cortex structure and function. *Nat Rev Neurosci* 10: 410–422.

86. Radley JJ, Rocher AB, Miller M, Janssen WGM, Liston C, Hof PR, *et al.* (2006): Repeated stress induces dendritic spine loss in the rat medial prefrontal cortex. *Cereb Cortex* 16: 313–320.

TABLES

ID	SEX	AGE	PMI	Diagnosis
NT1	Male	19	18.58	No clinical brain diagnosis found
NT2	Male	33	25.67	No clinical brain diagnosis found
NT3	Male	24	13.1	No clinical brain diagnosis found
NT4	Male	18	19.83	No clinical brain diagnosis found
NT5	Male	35	25.67	No clinical brain diagnosis found
TD1	Male	39	27	Tourette's disorder (Confirmed Diagnosis)
TD2	Male	8	12.3	Tourette's disorder (Confirmed Diagnosis)
TD3	Male	14	6.5	Tourette's disorder (Confirmed Diagnosis)
TD4	Male	29	19	Tourette's disorder (Confirmed Diagnosis)
TD5	Male	34	30.1	Tourette's disorder (Confirmed Diagnosis)

Table 1: Demographic and clinical characteristics of postmortem brain samples included in the study. The cohort comprised ten male subjects, aged 8 to 39 years, with postmortem intervals (PMI) ranging from 6.5 to 30.1 hours. Five subjects had no clinical brain diagnosis and served as controls, whereas five subjects had a confirmed diagnosis of Tourette's disorder based on clinical records and neuropathological verification. Post-mortem interval (PMI) was calculated as the time between death and brain freezing. All samples were obtained from male donors to minimize confounding effects of sex on gene expression.

Clusters	Overlap	P value	Odds ratio
Global	53	7.5845E-09	2.913379105
Pyramidal neurons	45	7.475E-09	3.114566705
Interneurons	28	0.026884042	1.564550114
Astrocytes	23	1.39909E-13	8.693377246
Oligodendrocytes	15	0.00011658	3.362769287
Oligodendrocyte precursor cells	13	2.61945E-11	15.32806613
Microglia	31	8.65096E-25	16.38797939

Table 2. Widespread enrichment of upregulated IEGs in DLPFC cell types in TD. All major dorsolateral prefrontal cortex (DLPFC) cell populations exhibited significant enrichment of upregulated immediate early genes (IEGs) in individuals with Tourette disorder (TD) compared with neurotypical controls, indicating broad activation of stress-responsive and transcriptionally induced pathways across both neuronal and glial lineages. The table summarizes the enrichment statistics for each cell class, including the number of overlapping upregulated IEGs (*Overlap*), the statistical significance of enrichment (*P* value, Fisher's exact test), and the *Odds ratio* representing the magnitude of enrichment.

FIGURES AND FIGURE LEGENDS

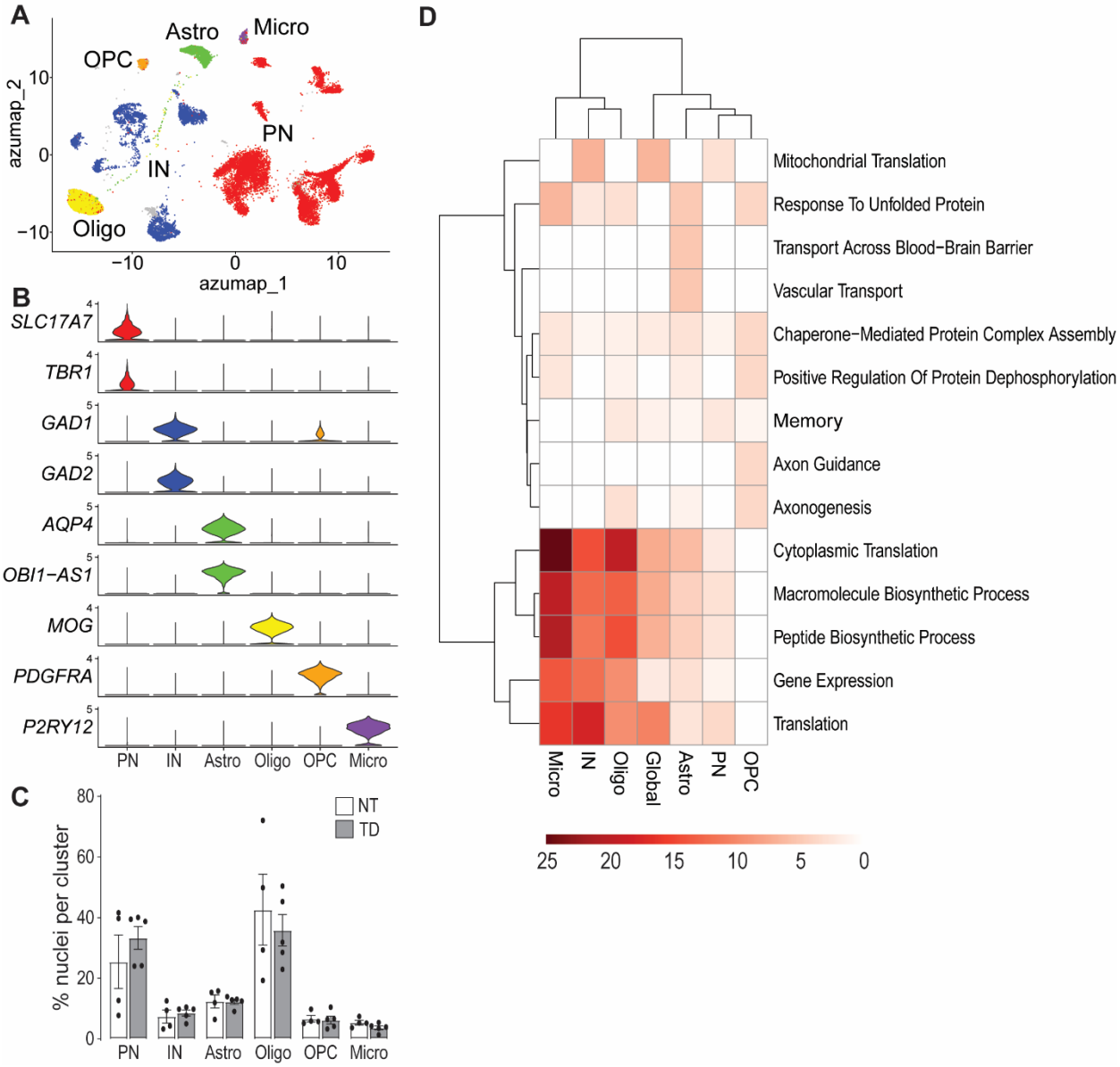

Figure 1: Single-nucleus transcriptomic profiling of BA9 tissues from neurotypical (NT) and Tourette Disorder (TD) patients. (A) Uniform Manifold Approximation and Projection (UMAP) following Azimuth projection on a BA9 reference, annotated by major cell types, including astrocytes, oligodendrocytes, microglia, pyramidal neurons, interneurons, and oligodendrocyte progenitor cells (OPC). (B) Violin plots of marker genes used to distinguish the clusters differentiating known cell types.

(C) Proportion of nuclei in each cluster, grouped by major cell type, for neurotypical and TD samples. (D) Gene ontology analysis for biological processes highlights the most differential biological processes among these cell clusters. Abbreviations: PN, pyramidal neurons; IN, interneurons; Astro, astrocytes; Oligo, oligodendrocytes; OPC, oligodendrocyte precursor cell; Micro, microglia.

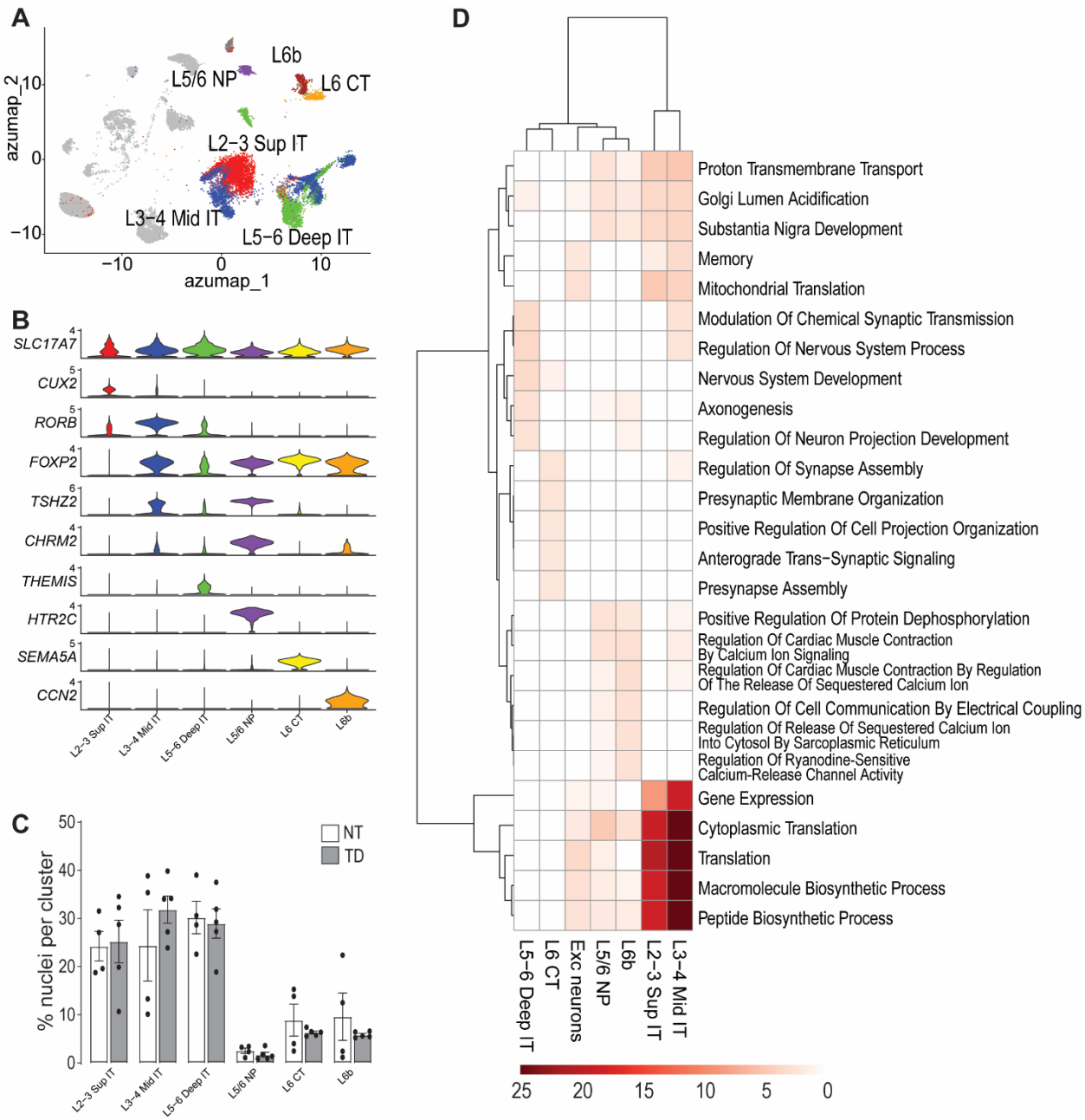

Figure 2: Cluster analysis of pyramidal neurons from neurotypical (NT) and Tourette Disorder (TD) patients. (A) Uniform Manifold Approximation and Projection (UMAP) visualization after Azimuth projection and annotated by major cell types. (B) Violin plots showing the expression of representative layer-specific marker genes used to define the clusters. (C) Proportion of nuclei in each cluster, grouped by major cell type, for NT and TD samples. (D) Gene ontology analysis for biological processes

highlights the most differential biological processes among these cell clusters. Abbreviations: L2-3 Sup IT, Layer 2-3 Superficial Intratelencephalic; L3-4 Mid IT, Layer 3-4 Middle Intratelencephalic; L5-6 Deep IT, Layer 5-6 Deep Intratelencephalic; L5/6 NP, Layer 5/6 Near-Projecting neurons; L6 CT, Layer 6 Corticothalamic; and L6b, Layer 6b.

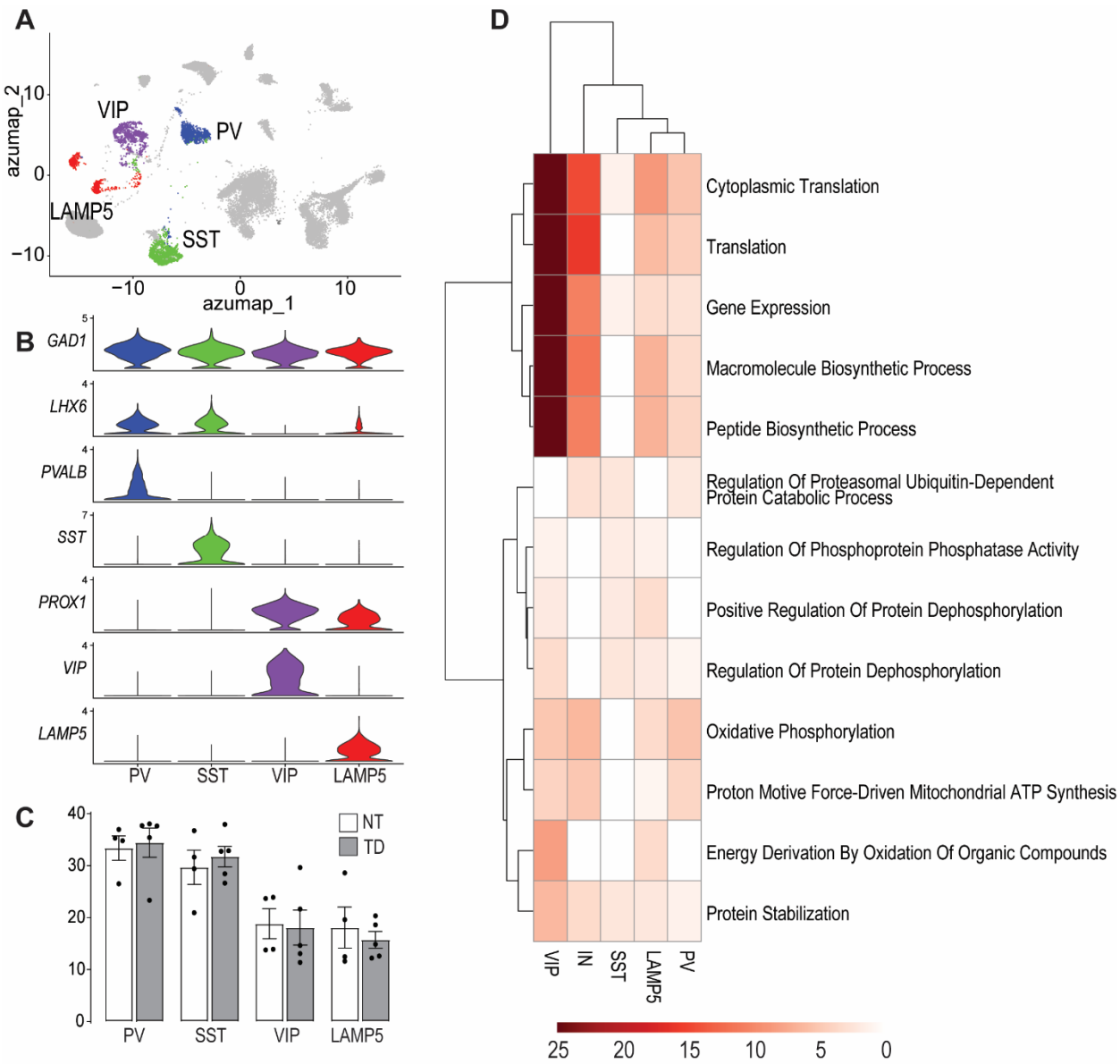

Figure 3: Cluster analysis of interneurons from neurotypical (NT) and Tourette Disorder (TD) patients. (A) Uniform Manifold Approximation and Projection (UMAP) visualization after Azimuth projection and annotated by major cell types. (B) Violin plots showing the expression of representative specific marker genes used to define the clusters. (C) Proportion of nuclei in each cluster, grouped by major cell type, for NT and TD samples. (D) Gene ontology analysis for biological processes highlights the most

differential biological processes among these cell clusters. Abbreviations: SST, somatostatin-positive; PV, parvalbumin-positive.

	Astro	PN	IN	Microglia	Oligo	OPC
Astro	36.41	1.30	1.01	0.91	0.00	1.82
PN	0.00	100.00	0.21	0.00	0.00	0.00
IN	0.00	0.38	30.54	0.00	0.00	0.51
Microglia	0.00	0.00	0.00	100.00	0.00	0.00
Oligo	0.54	0.00	0.00	0.00	100.00	3.25
OPC	0.00	0.00	3.64	0.00	0.00	38.22

Figure 4: Cross-dataset correspondence of cell-type cluster assignments. Odds ratios quantifying the correspondence between cell-type clusters identified in the present dataset (rows) and reference dataset annotations (columns). Higher odds ratios indicate stronger correspondence between clusters. Cell shading reflects the magnitude of the odds ratio, ranging from yellow (higher values) to blue (lower values). Cells outlined in red denote statistically significant associations after correction for multiple comparisons ($P < 0.001$). Abbreviations: Astro, astrocytes; PN, pyramidal neurons; IN, interneurons; Oligo, oligodendrocytes; OPC, oligodendrocyte precursor cells.

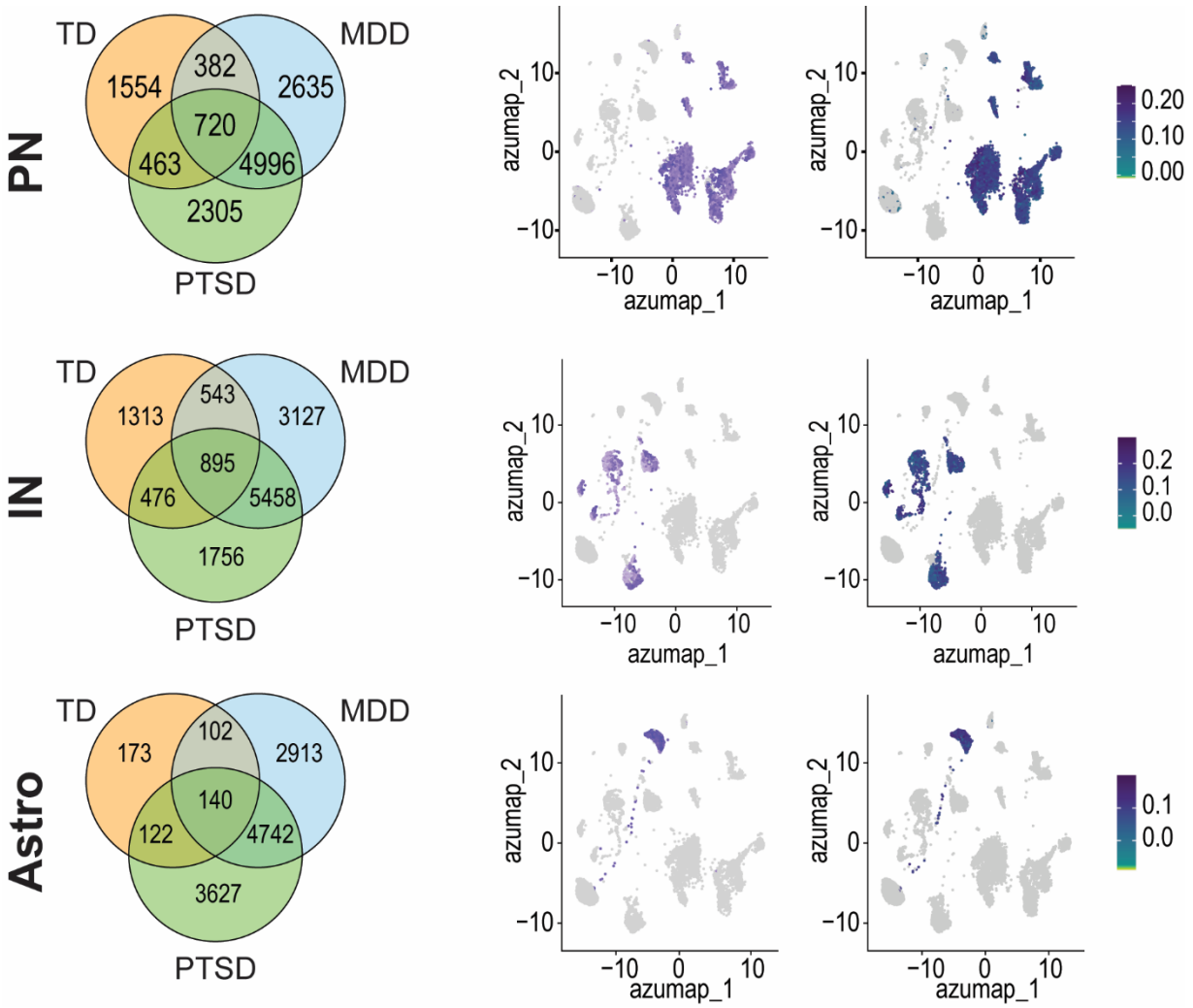

Figure 5. Cell-type–specific overlap between TD-, MDD-, and PTSD-associated transcriptional signatures and visualization of shared stress-responsive gene programs. Venn diagrams (left column) depict the intersection of upregulated genes identified in the DLPFC of individuals with TD and published single-nucleus transcriptomic datasets from major depressive disorder (MDD) and post-traumatic stress disorder (PTSD). Overlaps are shown separately for the following major cortical cell classes: pyramidal neurons (PN), interneurons (IN), and astrocytes (Astro). Each diagram illustrates the number of DEGs unique to each condition as well as the genes

shared across disorders, highlighting the substantial convergence of stress-related transcriptional programs between TD and these established stress-linked conditions.

The adjacent UMAP feature plots (center and right columns) display the distribution and relative expression intensities of the overlapping TD–MDD and TD–PTSD gene sets projected onto the integrated DLPFC single-nucleus transcriptomic atlas. Darker colors indicate higher average module scores within each cell, demonstrating that stress-responsive transcriptional programs shared with MDD and PTSD are enriched across multiple neuronal and glial populations in TD. Together, these analyses reveal a broad, multicellular convergence of stress- and glucocorticoid-associated gene expression signatures and underscore the engagement of stress-responsive pathways across the DLPFC in TD.

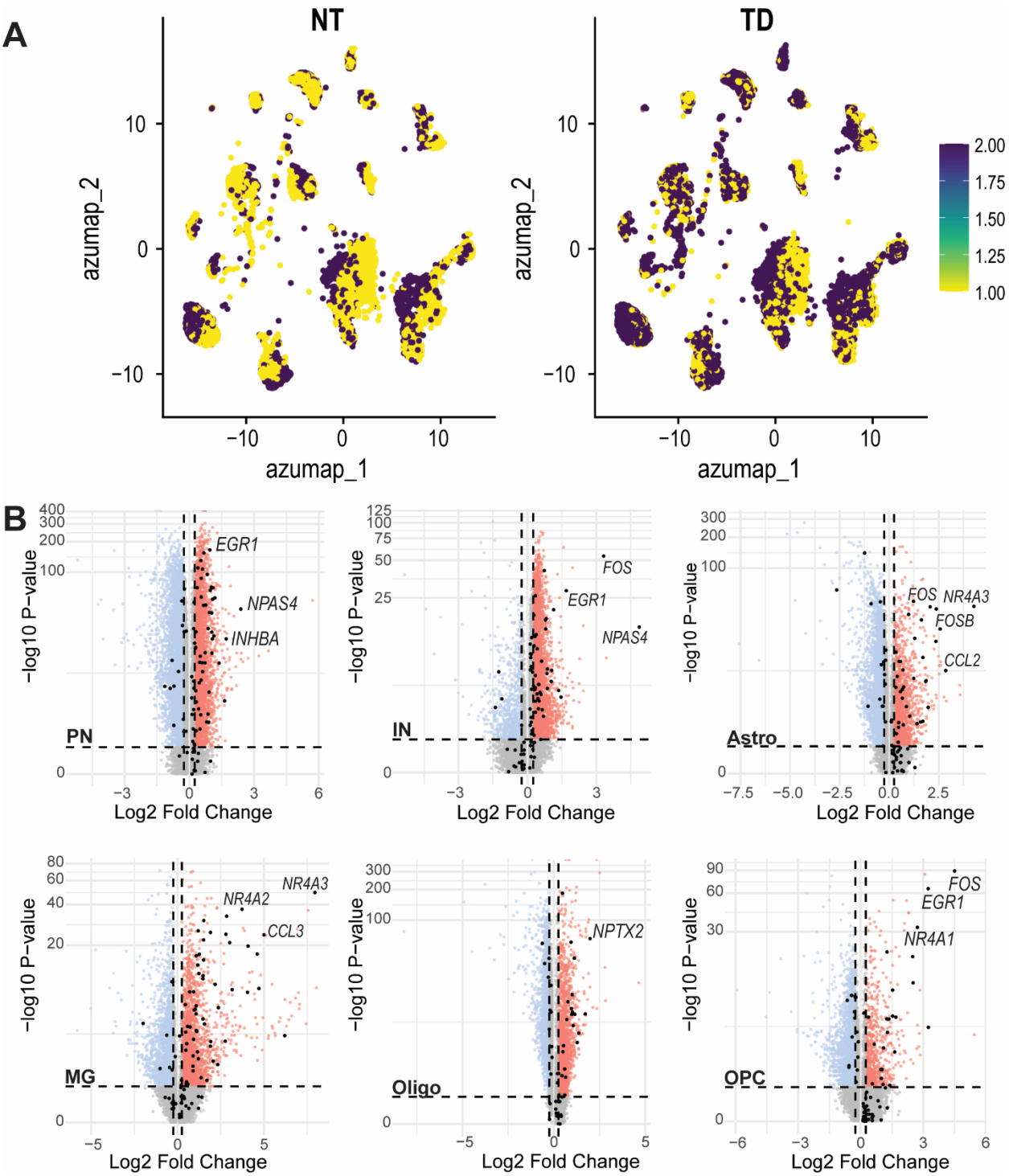

Figure 6. Cell-type-specific IEG activation signatures in Tourette disorder. (A) Dexamethasone-responsive gene module scores for neurotypical (NT) and Tourette disorder (TD) conditions. Colors represent module expression levels from low (yellow) to high (dark purple) based on dexamethasone-induced gene signatures derived from

Chatzinakos et al., 2023 (29). Each dot represents an individual cell positioned by transcriptional similarity. (B) Volcano plots showing differential gene expression analysis for six major brain cell types: pyramidal neurons (PN), inhibitory neurons (IN), astrocytes (Astro), microglia (MG), oligodendrocytes (Oligo), and oligodendrocyte precursor cells (OPC). X-axis displays $\log_2$ fold change (Tourette disorder vs. control), Y-axis shows $-\log_{10}$ P-value. Red dots denote significantly upregulated DEGs and blue dots denote significantly downregulated DEGs (FDR-adjusted $P < 0.05$, $|\log_2 FC| \geq 1.5$). Black dots indicate immediate early genes (IEGs), and gray dots represent genes that do not meet the significance or fold-change thresholds ($|\log_2 FC| < 1.5$ and $P \geq 0.05$). Key immediate early genes are labeled, including *EGR1*, *FOS*, *FOSB*, *NR4A3*, *NR4A2*, *CCL2*, *NPTX2*, and *NR4A1*. Dashed horizontal line represents $P = 0.05$ significance threshold; dashed vertical lines indicate ± 1.5 $\log_2$ fold change thresholds. IEG enrichment analysis conducted using curated reference gene set from Wu et al. 2017 (42).